Available online at www.sciencedirect.com

ScienceDirect

Ceramics International 40 (2014) 3261–3267

CERAMICS INTERNATIONAL

www.elsevier.com/locate/ceramint

Characterization of Mg-substituted hydroxyapatite synthesized by wet chemical method

Liga Stipniece[a,*], Kristine Salma-Ancane[a], Natalija Borodajenko[a], Marina Sokolova[b], Dmitrijs Jakovlevs[b], Liga Berzina-Cimdina[a]

[a]*Institute of General Chemical Engineering, Faculty of Materials Science and Applied Chemistry, Riga Technical University, Latvia*
[b]*Rudolfs Cimdins Riga Biomaterials Innovation and Development Centre, Latvia*

Received 25 June 2013; received in revised form 24 September 2013; accepted 24 September 2013
Available online 2 October 2013

Abstract

Mg-substituted hydroxyapatite made up of needle-like and plate-like particles containing different amounts of Mg (between 0.21 wt% and 2.11 wt%) were prepared via wet chemical precipitation method of a homogenous suspension of $Mg(OH)_2$/$Ca(OH)_2$ and an aqueous solution of H_3PO_4. According to the data of Brunauer–Emmett–Teller method and field emission scanning electron microscopy, high specific surface area Mg-substituted hydroxyapatite was obtained. Specific surface area of as-synthesized powders increased from 94.9 $m^2\ g^{-1}$ to 104.3 $m^2\ g^{-1}$ with increasing concentration of Mg up to 0.64 wt%. Fourier transform infrared spectroscopy, X-ray powder diffraction, differential thermal analysis, and heating microscopy, were used to evaluate thermal stability and sintering behavior of synthesis products. Increase in concentration of Mg in synthesis products ($\geq$0.83 wt%) promoted decomposition of Mg-substituted hydroxyapatite to Mg-substituted β-tricalcium phosphate after thermal treatment.

Keywords: Wet chemical precipitation; Hydroxyapatite; Mg substitution

1. Introduction

Hydroxyapatite (HAp, $Ca_{10}(PO_4)_6(OH)_2$) is one of the most attractive biomaterial for bone repair since it shows an excellent biological compatibility and osteoconductivity [1–3]. Modification of the chemical composition provides a simple but powerful approach in tailoring the properties of synthetic calcium phosphates (CaP). The study of ionic substitutions in HAp has been well recognized from the research reports due to the impending role of several micro-elements in the biological processes upon implantation [4]. Some authors reported the presence of magnesium (Mg) in calcified living tissues, suggesting that Mg ions might improve the biocompatibility and bioactivity of CaP ceramics [5–7].

Mg is one of the essential elements for all living organisms, *i.e.* 60–65% of total amount of Mg in a human body is found in bones and teeth, and the remaining 35–40% of Mg are scattered throughout the rest of the body, *i.e.* muscle tissues, nervous and other soft tissues, and body fluids. Mg participates in important functions of the body, including muscle activity by helping them to shrink and expand, nervous system and maintain a stable and strong heart rate [8]. Mg as well as Ca provide strong and healthy bones and reduce the risk of osteoporosis. Osteoporosis is described as an increased Ca "leaching" of bones caused by the lack of Mg. It is expected that Mg-substituted CaP (Mg–CaP) products used during bone repair surgery will ensure faster and more efficient recovery of the damaged bone by decomposition into environment of body and gradually releasing Mg ions. The physicochemical properties of the material will ensure progressive bone regeneration process until it is completely replaced by new bone. Despite

*Correspondence to: Institute of General Chemical Engineering, Faculty of Materials Science and Applied Chemistry, Riga Technical University, Azenes 14/24, Riga LV-1048, Latvia. Tel.: +371 22433769, +371 67089605; fax: +371 67089619.
E-mail addresses: liga.stipniece@rtu.lv, ligastipniece@inbox.lv (L. Stipniece).

0272-8842/$ - see front matter © 2013 Elsevier Ltd and Techna Group S.r.l. All rights reserved.
http://dx.doi.org/10.1016/j.ceramint.2013.09.110

the low concentrations (enamel, dentin and bone contain 0.44, 1.23 and 0.72 wt% of Mg, respectively) Mg has a decisive role on bone metabolism, especially in the early stages of an osteogenesis when it stimulates osteoblast proliferation. Deficiency of Mg causes bone loss [9,10].

Some works are reported in the literature since the 60's and 70's on synthesis of CaP containing Mg. The characters of products are widely different depending on the synthesis parameters including type of process, physicochemical properties of the reactants, concentrations, temperature, aging, *etc.* [11]. Cacciotti et al. in their researches discovered that the incorporation of Mg into HAp lattice sensibly affects apatite crystallization in solution and its thermal stability, promoting the formation of β-tricalcium phosphate (β-TCP, $Ca_3(PO_4)_2$) and thus forming biphasic calcium phosphates (BCP) [6]. Generally, ionic substitutions in the CaP structure could be made through wet chemical methods or solid-state routes. The maximal amount of Mg ions substituting for Ca ions into HAp structure have been obtained using wet chemical methods (*i.e.* wet chemical precipitation and hydrothermal synthesis). The Mg substituting of apatite often is performed by using an inorganic Mg source, such as $MgCl_2 \cdot 6H_2O$ [4], $Mg(NO_3)_2 \cdot 6H_2O$ [9] and $Mg(OH)_2$ [12]. In order to improve mechanical properties of the material, in most of the earlier studies, HAp bioceramics were doped with MgO without a substituting character. The present work reports the effectiveness of MgO in synthesizing Mg-substituted HAp (Mg–HAp) via the classical neutralization route involving CaO and H_3PO_4 precursors. The objective of this work is to synthesize Mg–HAp powders with different Mg contents, aimed to study the influence of Mg ions on physicochemical properties of HAp. The wet chemical method was selected on the basis of previous experience in the synthesis of un-substituted HAp powders [13].

2. Materials and methods

Mg–HAp powders were prepared through wet chemical method and subsequent thermal treatment at 1100 °C for 1 h, involving CaO (puriss., *Sigma-Aldrich*, Germany), MgO (reagent-grade, *ES/Scharlau*, Spain) and H_3PO_4 (puriss., 85%, *Sigma-Aldrich*, Germany) precursors. The starting suspensions of 0.15 M $Ca(OH)_2$ or $Mg(OH)_2/Ca(OH)_2$ was obtained by "lime slaking" process, *i.e.* CaO or mixtures of CaO/MgO was suspended in distilled water and homogenized by a planetary ball milling at 300 rpm for 40 min. Various concentrations of Mg in the products were provided by changing into synthesis media added amount of MgO. Sample designations and into synthesis media added amount of MgO in respect to total volume of CaO/MgO mixtures are summarized in Table 1. Aqueous solution of 2 M H_3PO_4 was added to the homogenous starting suspensions at a slow addition rate (~0.75 ml/min) under vigorous stirring. The temperature of synthesis media was maintained constant (45 °C). The pH was adjusted to 9 by adding 2 M H_3PO_4 solution and stabilized for 1 h. The obtained precipitates were aged in mother liquors at ambient temperature for ~20 h, filtered and finally dried at 105 °C for ~20 h (as-synthesized samples). Subsequent sintering of as-synthesized powders in an electrically heated furnace in air atmosphere at 1100 °C for 1 h followed (sintered samples).

Table 1
Samples designations, into synthesis media added amount of MgO and Mg concentrations of the samples sintered at 1100 °C for 1 h determined by EDS analysis.

Samples	Amount of MgO (wt%)	Mg concentration (wt%)
HAp	0	0.21 ± 0.02
1.0 Mg–HAp	1	0.43 ± 0.09
2.0 Mg–HAp	2	0.64 ± 0.10
3.0 Mg–HAp	3	0.83 ± 0.19
10.0 Mg–HAp	10	2.11 ± 0.27

The concentrations of Mg of the final samples were determined using energy dispersive X-ray spectroscopy (EDS, *Mira/LMUInca Energy* 350, Tescan, Czech Republic).

The thermal stability of as-synthesized samples was evaluated by differential thermal analysis (DTA, *Thermoanalyse GmbH DTA/DSC 703*, BÄHR, Germany) at a heating rate 10 °C/min from ambient temperature to 1400 °C.

The sintering of as-synthesized powders was investigated through dilatometric experiments by heating microscope (*EM*201 (*HT*-16 (1600/80), Hesse Instruments, Germany) using the following conditions: samples weighing ~20 mg was pressed into a cylindrically shaped pellets and heated to 500 °C at a heating rate 80 °C/min, and further to 1350 °C at 15 °C/min. Solution of isopropanol as a binder for obtaining pellets of as-synthesized powders was used.

The morphological features of as-synthesized powders and the microstructural features of sintered samples were studied by field emission scanning electron microscopy (FE-SEM, *Mira/LMU*, Tescan, Czech Republic) at acceleration voltage of 30 kV and a distance of 10 mm. Samples were sputter coated with a thin gold layer (thickness 15 nm) since CaP powders are electrically non-conductive. The micrographs of the ceramic samples were observed from the fracture surfaces. The samples were collected in the form of a suspension after stabilization period and dried at 105 °C for ~20 h to investigate the morphology of as-synthesized powders.

Various functional groups present in the Mg–HAp powders were identified by Fourier transform infrared spectroscopy (FT-IR, *Varian 800*, USA). Here 1 wt% of the powders were mixed and ground with 99 wt% KBr. The tablets of the powder mixtures of 13 mm diameter were pressed at 50 kN and the spectra were recorded in the range of 400–4000 cm^{-1} with spectral resolution 4 cm^{-1} and 50 times scanning.

The Brunauer–Emmett–Teller (BET) method was used to determine the specific surface area (SSA) of as-synthesized powders by N_2 adsorption (*Sorptometer KELVIN* 1042, USA). Powders were heated to 300 °C before analysis, to remove all the adsorbed water present in the apatite structure. The particle sizes of primary crystals were estimated from the N_2 adsorption isotherms using the BET particle diameter (d_{BET}) from the following equation by assuming the primary particles

to be spherical:

$$d_{BET} = 6/(qSw), \quad (1)$$

where q is density and Sw is the SSA. A density of 3.156 g/cm^3, which is a theoretical density of stoichiometric HAp, was used for all calculations [12].

X-ray diffraction analysis (XRD) was used to identify the crystalline phases over a 2θ range of 20–70° in a powder X-ray diffractometer (*PANalyticalX'Pert Pro*, The Netherlands) using Cu K_α ($\lambda = 1.5406$ Å) radiation produced at 40 kV and 30 mA with a step size of 0.0334°, and a counting time of 200.025 s. XRD analyses were performed on the as-synthesized powders

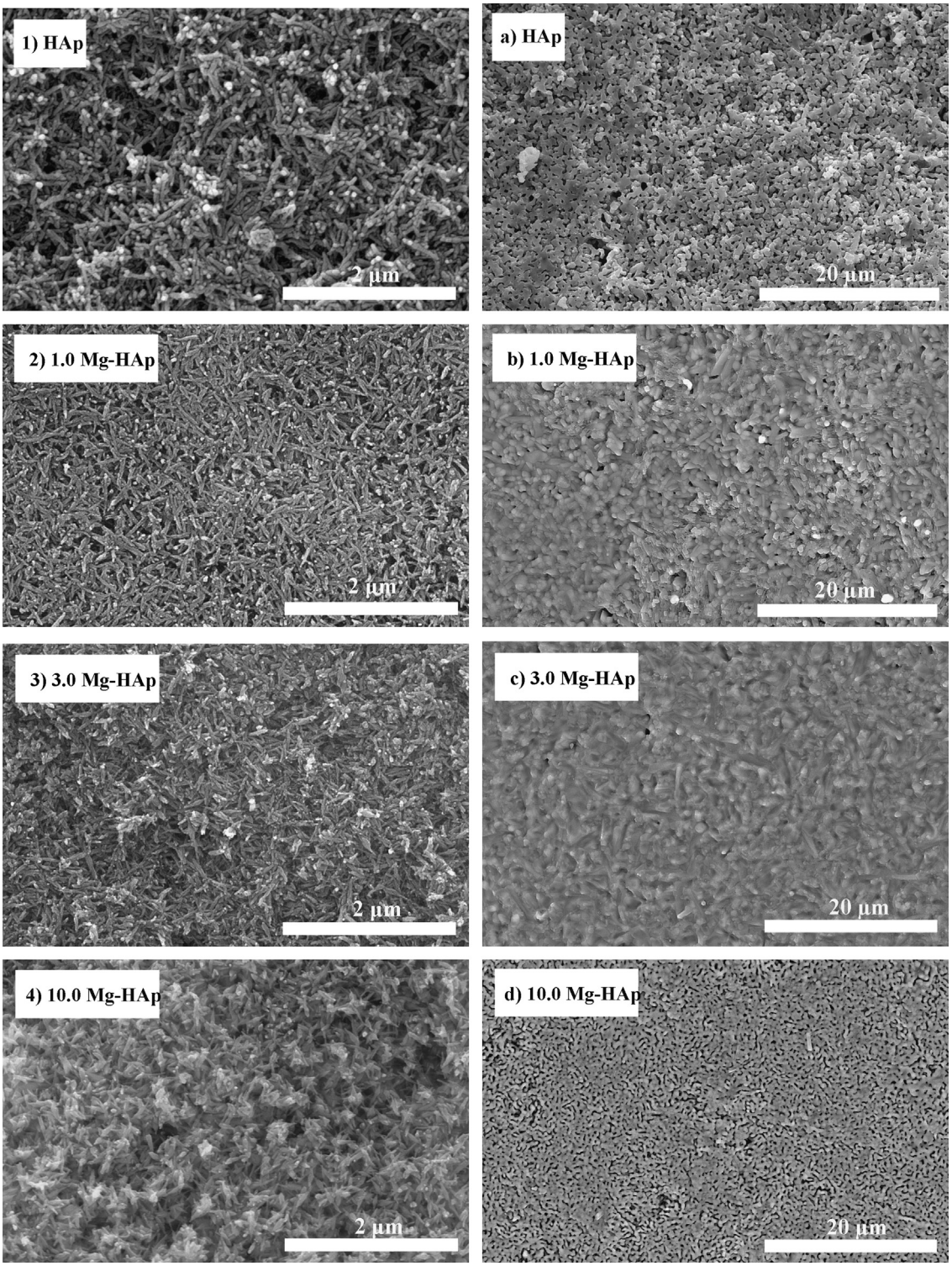

Fig. 1. FE-SEM microphotographs of as-synthesized powders (1–4) dried at 105 °C for 20 h and surface microstructures of ceramics (a–d) sintered at 1100 °C for 1 h.

as well as the powders after sintering at 1100 °C. For the phase identification *American Mineralogist Crystal Structure Database* (AMCDS) was used, which were card #0001257 for HAp, #0004624 for β-TCP and #0013351 for Mg-substituted β-TCP (Mg-β-TCP).

3. Results and discussion

The concentrations of Mg in the final samples measured by EDS are summarized in Table 1. The measurements of EDS indicated that HAp contain 0.21 wt% of Mg. This Mg content resulted from impurities in commercial CaO. The analyses of EDS showed the presence of Ca, P, Mg and O in all powders. The concentration of Mg in the synthesis products ranged between 0.21 wt% and 2.11 wt%. In general, EDS mapping indicated that Mg was uniformly dispersed in the CaP samples and Mg substitution level in the HAp increased proportionally with the MgO content in the starting slurry.

FE-SEM microphotographs showing the morphologies of as-synthesized powders and the microstructures of ceramics sintered at 1100 °C are reported in Fig. 1(1–4). Precipitates of HAp showed a typical nanosized, needle-like crystallite agglomerate morphology with homogenous, thin (elongated, ~150–200 nm) secondary crystallites (Fig. 1(1)). Mg–HAp precipitates indicated a needle-like and plate-like crystallite agglomerate morphology as shown in Fig. 1(2)–(4).

The SSA as well as the average particle sizes (d_{BET}) of the as-synthesized powders is presented in Table 2. The calculated d_{BET} ranged between 18 nm and 21 nm. According to literature, the SSA of the natural bone minerals are 87 $m^2\ g^{-1}$ [14] and 100 $m^2\ g^{-1}$ [15], which is of the same order of magnitude as the SSA of the as-synthesized Mg–HAp. However, the BET results could be affected by compact crystal aggregation. The similar values of SSA for the as-synthesized powders containing different amounts of Mg (in range between 0.21 wt% and 0.64 wt%) imply that in our case incorporation of Mg ions had only minor influence on crystal dimensions. The FE-SEM analyses combined with the SSA measurements indicated that the nanosized primary particles form agglomerates with each other. As the Mg content in the powders increased up to 2.11 wt%, crystallites became thinner and finer.

The XRD patterns of the as-synthesized powders are presented in Fig. 2. All as-synthesized products are characterized by a crystalline structure and a low crystallinity, as evidenced by XRD patterns with relatively broad and low-intensity XRD peaks. No significant differences in XRD data of as-synthesized powders were detected, even though their elemental analysis confirmed the presence of certain amounts of Mg substitutions. All XRD patterns marked triplets or broad, intense diffraction band ranging from 31.7° to 33.0° 2θ and individual intensive peak at 25.7° 2θ characteristic to an apatite phase. However, the samples designated as 3.0 Mg–HAp and 10.0 Mg–HAp shows peak shifts of the peaks located at 26°, 32°, 33°, 34° and 40° to a higher reflex angles. A shift in the diffraction peaks to a higher 2θ angle with increasing Mg content in Mg–HAp samples might indicate decreasing of *a*-axis dimensions of the crystallites [16]. Some authors related that the incorporation of Mg in the apatite lattice causes a reduction of a crystal size, a contraction in the *a*-axis dimension and an expansion in the *c*-axis dimension [17,18].

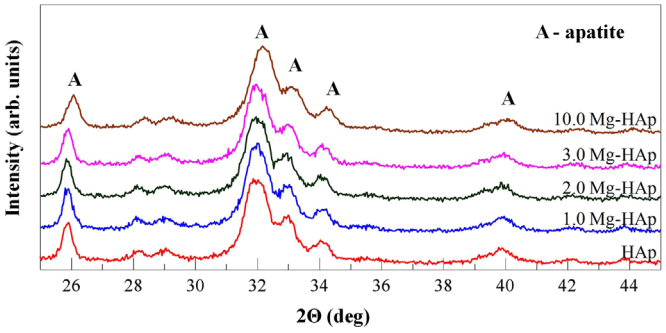

Fig. 2. XRD spectra of as-synthesized HAp, 1.0 Mg–HAp, 2.0 Mg–HAp, 3.0 Mg–HAp and 10.0 Mg–HAp powders dried at 105 °C for 20 h.

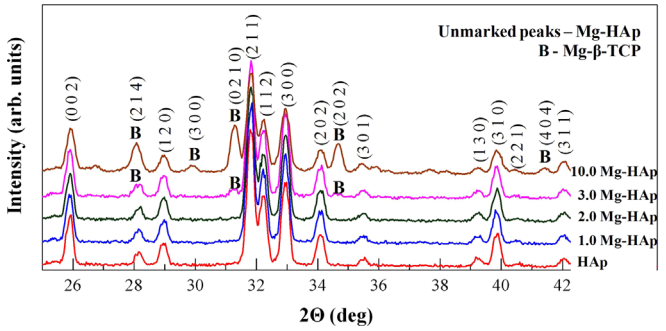

Fig. 3. XRD spectra of HAp, 1.0 Mg–HAp, 2.0 Mg–HAp, 3.0 Mg–HAp and 10.0 Mg–HAp powders sintered at 1100 °C for 1 h.

The powders were sintered at 1100 °C in order to investigate the effect of Mg incorporation on the thermal stability of HAp and HAp→β-TCP phase transition. Thermal treatment of as-synthesized powders resulted in narrowing of the XRD peaks, attributed to the increasing of crystallite size and crystallinity (Fig. 3). According to the literature [19], incorporation of Mg leads to a gradual transformation of Mg–HAp to Mg-β-TCP between 300 °C and 1100 °C, depending on the Mg content. The XRD peaks derived from both Mg–HAp and Mg-β-TCP were detected in the sintered samples containing 0.83 wt% and 2.11 wt% of Mg (3.0 Mg–HAp and 10.0 Mg–HAp, respectively), which indicates the formation of BCP ceramics. It is

Table 2
Specific surface area (SSA) and average particle size (d_{BET}) of as-synthesized powders.

Samples	SSA (m^2/g)	d_{BET} (nm)
HAp	94.9	20
1.0 Mg–HAp	101.6	19
2.0 Mg–HAp	104.3	18
3.0 Mg–HAp	100.2	19
10.0 Mg–HAp	91.0	21

generally difficult to distinguish between synthetic β-TCP and Mg-β-TCP phases due to the overlapping of characteristic peaks. However, it was observed that in the case of Mg-substituted CaP (Mg–CaP) products the 2θ values were much closer to those reported in AMCSD 0004624 (*American Mineralogist Crystal Structure Database*) for synthetic Mg-β-TCP than β-TCP. The thermal stability of Mg–HAp samples decreased and the transformation of HAp phase occurred while the Mg content (≥ 0.83 wt%) increased. Therefore, at higher content of Mg, Mg–HAp phase could be transformed to Mg-β-TCP phase, indicating the total amount of Mg-β-TCP in the samples increased, compared to the samples containing lower Mg content. It was observed by comparing the diffraction patterns obtained for each of sintered (at 1100 °C for 1 h) samples, *i.e.* relative intensities of peaks (2 1 4) at 27.90° 2θ, (0 2 1 0) at 31.13° 2θ and (2 2 0) at 34.49° 2θ characteristic of Mg-β-TCP.

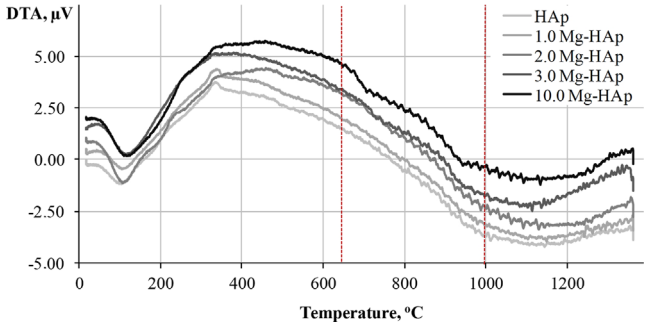

Fig. 4. DTA curves of HAp, 1.0 Mg–HAp, 2.0 Mg–HAp, 3.0 Mg–HAp and 10.0 Mg–HAp powders.

However, occupancy and behavior of Mg in the substituted biphasic mixtures cannot be determined quantitatively from the present results, which need an extensive structural investigation. These biphasic mixtures will be a welcome feature for a material to be applied in a biomedical applications as it is evidenced that BCP materials composed of a stable phase of HAp and a soluble phase of β-TCP in the various ratios show an ability to control the balance between the bioactivity and the solubility in the living body, which guarantees the stability of ceramics during the bone ingrown process [20].

From the XRD analyses it was confirmed that the single phase HAp with Mg substitution level up to 0.64 wt% and with maintained original crystalline structure was synthesized trough the wet chemical precipitation followed by the sintering at 1100 °C. It is likely to achieve a substitution of Mg into the structure of synthetic HAp resembled to those of bone mineral.

The DTA analyses (Fig. 4) of as-synthesized HAp and Mg–HAp powders are in a good agreement with the results of XRD analyses. The endothermic effect in temperature region

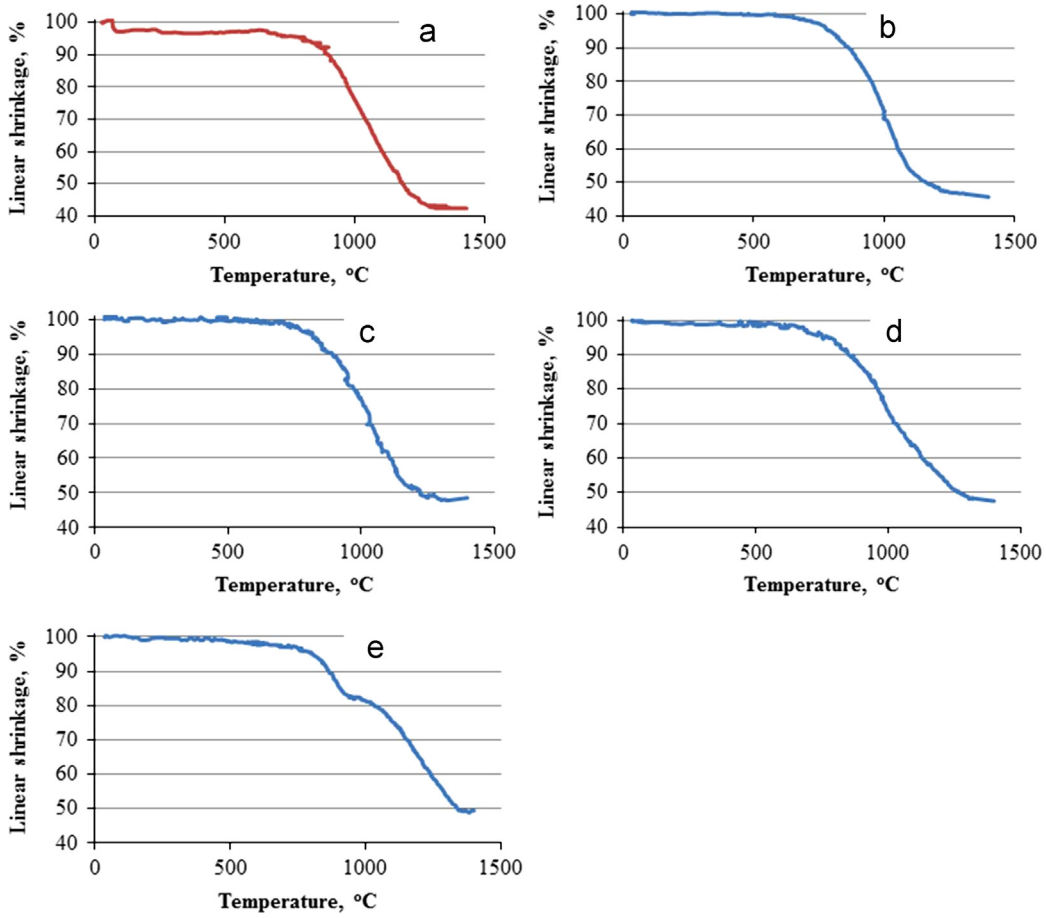

Fig. 5. Dilatometric curves of HAp, 1.0 Mg–HAp, 2.0 Mg–HAp, 3.0 Mg–HAp and 10.0 Mg–HAp powders.

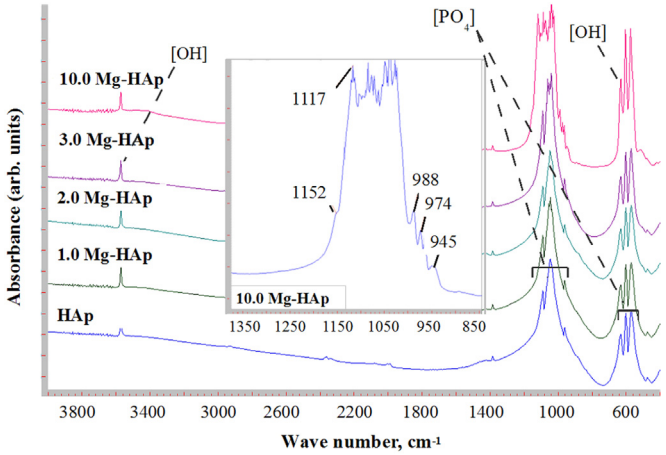

Fig. 6. FT-IR spectra of HAp, 1.0 Mg–HAp, 2.0 Mg–HAp, 3.0 Mg–HAp and 10.0 Mg–HAp powders sintered at 1100 °C for 1 h.

between 50 °C and 150 °C observed in all of the DTA curves is due to the removal of physically adsorbed H_2O and CO_2. The DTA curves of samples containing 0.21 wt%, 0.43 wt% and 0.64 wt% of Mg (HAp, 1.0 Mg–HAp, and 2.0 Mg–HAp, respectively) does not show any other endothermic peaks up to 1400 °C. In the case of samples containing 0.83 wt% and 2.11 wt% of Mg (3.0 Mg–HAp and 10.0 Mg–HAp, respectively), DTA curve shows some distortions in temperature region of 650–1000 °C. Those regions of DTA curves can be due to the decomposition of the Mg–HAp to Mg-β-TCP phase.

Similar results provide the HM measurements. The dilatometric curves and the linear shrinkage rate of the different samples are compared in Fig. 5, up to 1400 °C. The sintering process of HAp and Mg–HAp ceramics starts at temperature of ~650–700 °C. In the case of 10.0 Mg–HAp samples, it was observed that above 900 °C Mg–HAp decomposed. It can be reasonably associated to the beginning of the Mg-β-TCP phase's formation, which then overlapped to the starting of densification followed by sample uniform compaction. Results of the FE-SEM investigations of the Mg–HAp ceramics sintered at 1100 °C shows essential differences in the grain sizes and the microporosity (Fig. 1(a–d)). In an agreement with Ref. [21], the incorporation of Mg into HAp structure gains the density of Mg–HAp ceramics. The increase of Mg content in ceramics induced formation of elongated grains and augments densification stage. However, it was observed that due to the presence of secondary phase – Mg-β-TCP, in the case of 10.0 Mg–HAp samples containing 2.11 wt% of Mg, the microstructure was more microporous than the structures of other Mg–HAp ceramics.

The FT-IR spectra of the sintered samples differ significantly from the FT-IR spectra of the as-synthesized samples. All spectra have intensive characteristic bands of HAp, originating from vibrations of $[PO_4]$ groups and bands corresponding to the stretching and vibrational modes of the [OH] (Fig. 6). Thus, broadening and splitting of characteristic absorption band of $[PO_4]$ groups were observed as the Mg content of sintered samples increased. In the case of samples with Mg content 2.11 wt% (10.0 Mg–HAp), extra peaks at

Table 3
The observed absorption peaks in the FTIR spectra of Mg–HAp and Mg-β-TCP sintered at 1100 °C for 1 h.

Assignment	Wave numbers (cm^{-1})	
	Mg–HAp	Mg-β-TCP
$[PO_4]$ ν_2	475	436
$[PO_4]$ ν_4	575	554
$[PO_4]$ ν_4	603	593; 603
$[PO_4]$ ν_1	963	945
$[PO_4]$ ν_3	1000–1200	974; 1038; 1105; 1117
[OH]	3569	–
[OH]	632	–

945, 974, 988, 1117 and 1152 cm^{-1} were detected, which is ascribed to the $[PO_4]$ vibration modes characteristic of Mg-β-TCP. Experimentally determined characteristic FT-IR peaks of Mg–HAp and Mg-β-TCP prepared by wet chemical precipitation method with subsequent sintering at 1100 °C for 1 h are summarized in Table 3.

4. Conclusions

In this study 0.21, 0.43, 0.64, 0.83 and 2.11 wt% Mg-substituted hydroxyapatite were prepared successfully through wet chemical method and subsequent sintering at 1100 °C for 1 h of CaO, H_3PO_4 and using MgO as substituting source. The as-synthesized powders, with specific surface areas over the range of 91.0–104.3 m^2/g, consisted of needle-like and/or plate-like crystalline particles. Increasing concentration of Mg into synthesis products contributed to a partial thermal decomposition of Mg-substituted hydroxyapatite to Mg-substituted β-tricalcium phosphate occurring in the temperature region from 650 °C to 1000 °C. Presence of Mg-substituted β-tricalcium phosphate into hydroxyapatite ceramic significantly changed its microstructure after thermal treatment which was distinctly different from microstructure of single phase Mg-substituted hydroxyapatite ceramic.

Acknowledgment

This work was supported by the Latvian State Research Program “Development of Innovative Multifunctional Materials, Signal Processing and Information Technology for Competitive Science Intensive Products” Project no. 4 “New Materials and Technologies for Evaluating Biological Tissue, and Replace”.

References

[1] S.V. Dorozhkin, Nanodimensional and nanocrystallinapatites and other calcium orthophosphates in biomedical engineering, biology and medicine, Materials 2 (4) (2009) 1975–2045.
[2] M. Vallet-Regí, J.M. González-Calbet, Calcium phosphates as substitution of bone tissues, Progress in Solid State Chemistry 32 (2004) 1–31.
[3] S.V. Dorozhkin, E. Matthias, Biological and medical significance of calcium phosphates, Angewandte Chemie International Edition 41 (2002) 3130–3146.

[4] E. Landi, G. Logroscino, L. Proietti, A. Tampieri, M. Sandri, S. Sprio, Biomimetic Mg-substituted hydroxyapatite: from synthesis to in vivo behaviour, Journal of Materials Science: Materials in Medicine 19 (2008) 239–247.
[5] J. Kolmas, A. Jaklewicz, A. Zima, M. Bucko, Z. Paszkiewicz, J. Lis, A. Slosarczyk, W. Kolodziejski, Incorporation of carbonate and magnesium ions into synthetic hydroxyapatite – the effect on physicochemical properties, Journal of Molecular Structure 987 (2011) 40–50.
[6] I. Cacciotti, A. Bianco, M. Lombardi, L. Montanaro, Mg-substituted hydroxyapatite nanopowders: synthesis, thermal stability and sintering behaviour, Journal of the European Ceramic Society 29 (2009) 2969–2978.
[7] T.-W. Kim, H.-S. Lee, D.-H. Kim, H.H. Jin, K.-H. Hwang, J.-K. Lee, H.-C. Park, S.-Y. Yoon, In situ synthesis of magnesium-substituted biphasic calcium phosphate and in vitro biodegradation, Materials Research Bulletin 47 (2012) 2506–2512.
[8] W. Mroz, A. Bomblaska, S. Burdynska, M. Jedynski, A. Prokopiuk, B. Budner, A. Slosarczyk, A. Zima, E. Menaszek, A. Scislowska-Czarnecka, K. Niedzielski, Structural studies of magnesium doped hydroxyapatite coatings after osteoblast culture, Journal of Molecular Structure 977 (2010) 145–152.
[9] D. Laurencin, N. Almora-Barrois, N.H. De Leeuw, C. Gervais, C. Bonhomme, F. Mauri, W. Chrzanowski, J.C. Knowles, R. J. Newport, A. Wong, Z. Gan, M.E. Smith, Magnesium incorporation into hydroxyapatite, Biomaterials 32 (2011) 1826–1837.
[10] J.M. Arnaud, Update on the assessment of magnesium status, British Journal of Nutrition 99 (2009) S24–S36.
[11] P.T. Cheng, J.J. Grabber, R.Z. LeGeros, Effects of magnesium on calcium phosphate formation, Magnesium 7 (3) (1988) 123–132.
[12] W.L. Suchanek, K. Byrappa, P. Shuk, R.E. Riman, V.F. Janas, K.S. TenHuisen, Preparation of magnesium-substituted hydroxyapatite powders by the mechanochemical–hydrothermal method, Biomaterials 25 (2004) 4647–4657.
[13] K. Salma, N. Borodajenko, L. Berzina-Cimdina, Calcium phosphate bioceramics prepared from wet chemically precipitated powders, Processing and Application of Ceramics 4 (1) (2010) 45–51.
[14] D.N. Misra, R.L. Bowen, G.J. Mattamal, Surface area of dental enamel, bone, and hydroxyapatite: chemisorption from solution, Calcified Tissue Research 26 (1978) 139–142.
[15] N.V. Wood, Specific surfaces of bone, apatite, enamel and dentine, Science 105 (1947) 531–532.
[16] M.A. Sader, K. Lewis, G.A. Soares, R.Z. LeGeros, Simultaneous incorporation of magnesium and carbonate in apatite: effect on physico-chemical properties, Materials Research 16 (4) (2013) 779–784.
[17] M. Okazaki, R.Z. LeGeros, Crystallographic and chemical properties of Mg-containing apatites before and after suspension in solution, Magnesium Research 5 (1992) 103–108.
[18] E. Landi, A. Tampieri, M.M. Belmonte, G. Celotti, M. Sandri, A. Gigante, et al., Biomimetic Mg- and Mg, CO_3-substituted hydroxyapatites: synthesis, characterization and in vitro behaviour, Journal of the European Ceramic Society 26 (2005) 2593–2601.
[19] A.K. Khanra, H.C. Jung, S.K. Yu, K.S. Hong, K.S. Shin, Microstructure and mechanical properties of Mg–HAp composites, Bulletin of Materials Science 33 (2010) 43–47.
[20] Z.Z. Zyman, M.V. Tkachenko, D.V. Polevodin, Preparation and characterization of biphasic calcium phosphate ceramics of desired composition, Journal of Materials Science: Materials in Medicine 19 (2008) 2819–2825.
[21] S.J. Kalita, H.A. Bhatt, Nanocrystalline hydroxyapatite doped with magnesium and zinc: synthesis and characterization, Materials Science and Engineering C 27 (2007) 837–848.